Engineering Design Methods for Cavitation Reactors II: Hydrodynamic Cavitation

Parag R. Gogate and Aniruddha B. Pandit

Chemical Engineering Section, University Dept. of Chemical Technology, Matunga, Mumbai-400 019, India

The bubble behavior and hence the pressure generated at the collapse of the cavity for hydrodynamic cavitation depends on the operating conditions and geometry of the mechanical constriction generating cavitation. The effect of operating parameters such as inlet pressure through the system's orifice, initial cavity size, and the indirect effect of the hole diameter (it affects the frequency of turbulence in the vicinity of the orifice) on the bubble behavior was numerically studied. The bubble dynamics were simulated in two stages considering: Rayleigh-Plesset equation up to the point of bubble wall velocity = 1,500 m/s; then the compressibility of the medium using the equation of Tomita and Shima. An empirical correlation was developed to predict the collapse pressure generated as a function of just mentioned parameters. The trends in the magnitudes of collapse pressure match the observed experimental trends for cavitation-induced reactions. The work is an extension of the earlier analysis done for the sonochemical reactors. Some recommendations are also suggested for the design of hydrodynamic cavitation reactors based on the simulations.

Introduction

Cavitation as a source of energy input for chemical processing is increasingly being studied because of its ability to generate localized high temperatures and pressures (hotspots) under nearly ambient conditions. The possibility of successful exploitation stems from the fact that millions of cavities grow and collapse simultaneously at different locations. Until now, ultrasound was the main method used for generating cavitation, and it has been extensively studied over the past few decades. In this method, passage of ultrasound through the cavitating medium generates cavities, promotes their growth, and their collapse. The whole process of cavity generation, growth, and collapse occurs over an extremely short period of time (microseconds). In spite of extensive research, there is hardly any chemical processing carried out on an industrial scale using ultrasound due to the expertise required in diverse fields, such as chemical engineering, material science, and acoustics, for scaling up the lab scale processes. In an earlier work (Gogate and Pandit, 2000), engineering design methods for the acoustic cavitational reactor were suggested. The present work aims at developing a similar technique for hydrodynamic cavitational reactors.

Hydrodynamic cavitation is a cheaper and simpler alternative for the ultrasound-based transformation processes (Senthilkumar et al., 2000). Here cavitation is generated by the flow of liquid through a simple geometry such as venturi tubes or orifice plates under controlled conditions. When the pressure at the throat falls below the vapor pressure of the liquid, the liquid flashes, generating a number of cavities, which subsequently collapse when the pressure recovers downstream of the mechanical constriction. A number of studies made earlier, such as hydrolysis of fatty oils (Pandit and Joshi, 1993), cell disruption using hydrodynamic cavitation (Save et al., 1997), polymerization/depolymerization of aqueous polymeric solutions (Chivate and Pandit, 1995), proved the process to be more energy efficient than its counterpart, acoustic cavitation. Modeling of a hydrodynamic cavitation system can aid in understanding the nature of the process and also in optimizing the operating parameters as well as the geometry of the hydrodynamic cavitation setup. The present work aims at modeling the magnitude of the pressure pulse generated at the time of collapse of the cavity. The collapse pressure will be dependent on the number of operating and geometrical conditions existing in the reactor, such as the inlet pressure, flow area of the orifice (diameter of the

hole and also the number of holes), and initial radius of the nuclei. Variation in the collapse pressure due to these parameters has been studied using rigorous numerical simulations and a generalized correlation has been developed for the prediction of the collapse pressure, which will help the design engineers in the design of a hydrodynamic cavitation setup.

Mathematical Modeling of Hydrodynamic Cavitation

Senthilkumar and Pandit (1999) have described in detail the modeling of hydrodynamic cavitation for a venturi type of system and also for the high-speed homogenizer. Moholkar and Pandit (1997) have modeled the hydrodynamic cavitation setup where flow takes place through the orifice, inserted inside the pipe, but considered the cavitating medium to be incompressible. The model described in the present work is an extension of the 1997 model, only with the medium considered compressible. The stepwise development of the turbulence model for the hydrodynamic cavitation is described in the following subsections.

Cavitation number (C_v)

Cavitation number is an important parameter in hydrodynamic cavitation. It can be expressed as,

$$C_v = \frac{p_2 - p_v}{\frac{1}{2}\rho_l v_o^2}, \tag{1}$$

where P_2 is the recovered pressure downstream of the orifice, p_v is the vapor pressure of the liquid, v_o is the average velocity of liquid at the orifice, and ρ_l is the density of the liquid.

Under ideal conditions, cavitation occurs for $C_v < 1$. This is also confirmed by the simulations performed in the present work, where the cavities generated oscillate continuously but do not collapse, for the value of $C_v > 2$. A typical profile of the variation of radius ratio with time is shown in Figure 1, where the generated cavity goes through the continuous cycles of expansion and contraction without collapsing. Also for the same condition, the magnitude of the pressure pulses generated is also quite small, which is evident in Figure 2. At this condition, the pressures generated by the collapse of cavities will not have any desired chemical effect, though it may
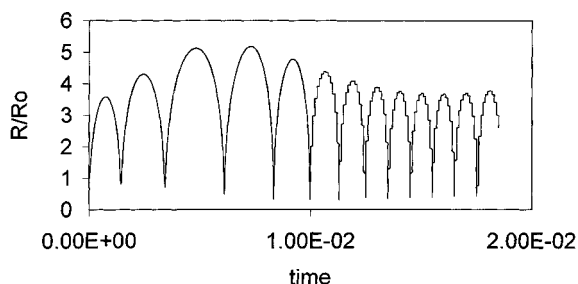

Figure 1. Variation of radius ratio with time for cavitation number > 2 indicating no collapse of cavities.
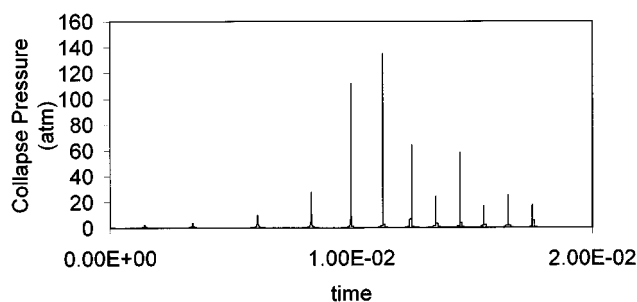

Figure 2. Variation of pressure pulse with time for high cavitation numbers typically greater than 2.

contribute a little to the mechanical and/or physical effects in the hydrodynamic cavitation setup. Thus such a condition must be avoided as far as possible, which can be checked by the resulting values of the cavitation number. But it also should be noted at this stage that the cavitation phenomena can also occur at C_v values greater than 1. This is due to the presence of dissolved gases or suspended particles in the liquid, which act as weak spots in the liquid providing nuclei for cavitation. The cavitation number is found to be a function of flow geometry (Yan and Thorpe, 1990; Vichare et al., 2000a) and in general, cavitation inception number increases with the diameter of the holes in the orifice plate.

Turbulence model

As the liquid flows through the orifice, due to reduction in the cross-sectional area of the flowing stream, the velocity head increases at the expense of the pressure head. During reexpansion, the flow gets separated at the lower end of the orifice and eddies are generated. The motion of the eddies causes turbulence and large friction losses occur. So permanent pressure loss is inevitable and full pressure recovery does not take place.

A turbulence model is used to predict the instantaneous pressure field around the traveling cavity at any downstream location and is analogous to that proposed by Moholkar and Pandit (1997) and Senthilkumar and Pandit (1999). The results of turbulence modeling and the fluctuating pressure field can be incorporated into a bubble dynamics equation to obtain the cavity radius history and the collapse pressures for a cavity of a certain size, traveling with the fluid.

In the case of turbulent flow, instantaneous velocity in the X-direction is given as,

$$v_x = \bar{v}_x + v'_x, \tag{2}$$

where $\bar{v}_x$ is the time averaged velocity at any point in the X-direction in the flowing liquid, and v'_x is the instantaneous fluctuating velocity. The amplitude of the fluctuating velocities in the X-direction can be expressed as mean of the squares of the fluctuation velocities $(\bar{v}'_x)^2$. Similar treatment can be given to the velocity fluctuations in other directions, that is, the Y- and Z-directions. The turbulent kinetic energy per unit mass of liquid is given as follows:

$$KE = -\frac{1}{2}\left[\left(\bar{v}'_x\right)^2 + \left(\bar{v}'_y\right)^2 + \left(\bar{v}'_z\right)^2\right]. \tag{3}$$

Power dissipated per unit mass of the liquid or the rate of loss of kinetic energy due to turbulence is as follows:

$$P_M = -\frac{1}{2} \frac{d}{dt} \left[(\bar{v}'_x)^2 + (\bar{v}'_y)^2 + (\bar{v}'_z)^2 \right]. \tag{4}$$

For isotropic turbulence, $\bar{v}'_x = \bar{v}'_y = \bar{v}'_z = \bar{v}'$;

$$\therefore P_M = -\frac{3}{2} \frac{d}{dt} (\bar{v}')^2. \tag{5}$$

For the estimation of fluctuating velocity $(\bar{v}')$ it is necessary to estimate the eddy length scale and the power dissipation per unit mass as for the case of isotropic turbulence, eddy length scale (Eq. 1), and the fluctuating velocity $(\bar{v}')$ can be related to P_M as follows,

$$P_M = \frac{(\bar{v}')^3}{l}. \tag{6}$$

In this section the stepwise estimation of the length scale and the power dissipation per unit mass are explained briefly. The details of the estimation of fluctuating velocities also were explained in the earlier work (Moholkar and Pandit, 1997; Senthilkumar and Pandit, 1999).

Medium-size eddies make more contribution to the kinetic energy and are commonly known as energy-containing eddies. Because the Prandtl eddy is a medium-size eddy, it is selected for the analysis. The eddy length scale is given as follows (Davies, 1972):

$$l = 0.08 \, d_x, \tag{7}$$

where d_x is the diameter of the conduit through which the liquid flows.

To account for the variation in the orifice and pipe diameters, the average of the length scales at the orifice and pipe has been considered:

$$l = 0.08 \left(\frac{d_o + d_p}{2} \right). \tag{8}$$

This consideration of the average eddy length scale is a modification done in the previous model (Moholkar and Pandit, 1997), which is more correct due to the fact that the liquid experiences two levels of turbulence: one passing through the pipe, and the other when it encounters a sudden constriction at the hole in the orifice plate.

The dominant frequency of turbulence thus can be given as

$$f_T = \frac{\bar{v}'}{l}. \tag{9}$$

The power input per unit mass of the system is equal to the rate of energy dissipation per unit mass of the liquid, and it is estimated by considering the permanent pressure head loss across the orifice. The rate of energy dissipation due to eddy losses is the product of the head loss and the volumetric

flow rate. Frictional pressure drop downstream of the orifice can be calculated as

$$\Delta p = \frac{4 f_r L_r v_t^2 \rho_l}{d_p}, \tag{10}$$

where f_r is the friction factor, L_r is the length of pressure recovery zone, d_p is the diameter of pipe, and V_t is the velocity of fluid downstream of the orifice. The friction factor depends on the Reynolds number (N_{Re}). For turbulent flow through pipes, f_r is given as follows (Davies, 1972):

$$f_r = \frac{0.079}{(N_{Re})^{0.25}}. \tag{11}$$

Equation 10, along with the definitions of the liquid velocity at the orifice and the actual turbulent velocity existing at any point downstream of the orifice, can be used to estimate the pressure at that point that is used in the simulations, as described later.

Single-cavity dynamics

The Rayleigh-Plesset equation for bubble dynamics is

$$R \left(\frac{d^2 R}{dt^2} \right) + \frac{3}{2} \left(\frac{dR}{dt^2} \right) = \frac{1}{\rho_l} \left[p_i - \frac{4\mu}{R} \left(\frac{dR}{dt} \right) - \frac{2\sigma}{R} - p_\infty \right], \tag{12}$$

where P_∞ is the turbulent pressure existing downstream of the orifice, which is given as

$$P_\infty = P_v + \frac{1}{2} \rho \{ v_o^2 - v_{td}^2 \} - \Delta P, \tag{13}$$

where v_o is the velocity of the liquid at the orifice, and v_{td} is the actual turbulent velocity at any point downstream of the orifice.

Velocity at the orifice can be calculated as

$$v_o = \frac{v_p}{n \beta^2}, \tag{14}$$

where v_p is the pipe inlet fluid velocity, β is the orifice-to-pipe-diameter ratio, and n is the number of holes in the plate. Also the actual turbulent velocity at any point downstream of the orifice is given by the following equation:

$$v_{td} = v_t + \bar{v}' \sin (2\pi \, f_T \, t) \tag{15}$$

A completely gaseous cavity has been considered. For the numerical simulations, growth of the cavity was considered to be isothermal in the initial stages, and Flynn's assumption (Flynn, 1964) was considered during the later stages of collapse. According to this assumption, the collapse of the cavity becomes adiabatic when the partial pressure of the gas inside the cavity equals the liquid medium vapor pressure. So transition from isothermal collapse to adiabatic collapse takes place when Flynn's criterion is satisfied.

The preceding equation is valid until the bubble wall velocity is less than 1500 m/s (the speed of sound in water), which considers the incompressible nature of the cavitating media. This assumption underestimates the collapse pressure generated during the adiabatic collapse phase of the bubble (Gogate and Pandit, 2000). To overcome this, compressibility of the medium was considered, and the external pressure was considered to be time dependent. The equation used for the simulations was developed by Shima and Tomita (1979) and Tomita and Shima (1986) and is as follows:

$$R\ddot{R}\left(1 - \frac{2\dot{R}}{C} + \frac{23\dot{R}^2}{10C^2}\right) + \frac{3}{2}\dot{R}^2\left(1 - \frac{4\dot{R}}{3C} + \frac{7\dot{R}^2}{5C^2}\right)$$
$$+ \frac{1}{\rho l}\left[\begin{array}{c} p_\infty(t) - p_2(r=R) + \frac{R}{C}\left(\dot{p}_\infty(t) - \dot{p}_{1(r=R)}\right) + \\ \frac{1}{C^2}\left\langle \begin{array}{c} -2R\dot{R}\left(\dot{p}_\infty(t) - \dot{p}_{1(r=R)}\right) + \frac{1}{2}\left(p_\infty(t) - \right. \\ p_{1(r=R)}\right)\left(\dot{R}^2 + \frac{3}{\rho l}\left(p_\infty(t) - p_{1(r=R)}\right)\right) \end{array}\right\rangle \end{array}\right]$$
$$= 0, \quad (16)$$

where p_1 and p_2 as a function of R are given as follows:

$$p_{1(r=R)} = p_v + p_{go}\left(\frac{R_o}{R}\right)^{3\gamma} - \frac{2\sigma}{R} - \frac{4\mu}{R}\dot{R} \quad (17)$$

$$p_{2(r=R)} = p_{1(r=R)} - \frac{4\mu}{3\rho C^2}\left(\dot{p}_{\infty(t)} - \dot{p}_{1(r=R)}\right). \quad (18)$$

Since the compressibility of the medium has been considered, it is not necessary to terminate the simulations when the bubble wall velocity exceeds 1500 m/s, but was terminated at the point where the R/R_o ratio becomes less than 0.1 (near complete collapse). Thus in the present simulations, the Rayleigh-Plesset equation was used for the range of bubble wall velocities less than 1,500 m/s, and the equation given by Tomita and Shima (1986) was used when this velocity exceeds 1,500 m/s. The effect and importance of consideration of the compressibility of the cavitating medium was explained well in our earlier work for the acoustic cavitation (Gogate and Pandit, 2000), as well as in the preliminary work carried out for the hydrodynamic cavitation (Tatake et al., 1999). It should be noted at this stage that the present model considers the estimation of the collapse pressures at the condition of a single cavity, and there are large numbers of cavities that are formed during the phenomena of cavitation. This case can be applied to the realistic situation by estimating the number of cavities that are formed and then calculating the total pressure pulse by multiplying the magnitude of pressure generated by the collapse of a single cavity with the number of cavities formed in the reactor. Sochard et al. (1998) and Prasad Naidu et al. (1994) have given a detailed analysis of the estimation of the number of cavities formed and active at any instance. Preliminary results have also indicated that the difference between the values of the pressure pulses obtained in the preceding two ways, that is, one assuming the cluster of cavities, and the other where a single cavity is considered and then multiplied with the number of cavities to get the resultant pressure pulse, is not significant.

Results and Discussion

Collapse pressure can be defined as the magnitude of the pressure pulse generated at the end of the collapse of the cavity. In the present case, the collapse of the cavity is assumed to be complete when the radius of the cavity is 0.1 times the original radius. The contribution of the adiabatic phase to the overall pressure pulse is maximum, and hence the simulations are terminated when $R/R_o = 0.1$, and not at the critical radius (Flynn's radius), where the collapse is completely isothermal. The effect of the various operating parameters, such as the inlet pressure and initial size of the nuclei in the system, on the final collapse pressure has been studied numerically. The size of the nuclei can be adjusted by changing the type of cavitating medium and the system, that is, dissolved gases, temperature, and concentration of species, which changes the vapor pressure. The diameter of the orifice and the percentage of free area occupied by the holes also affect the magnitude of the collapse pressure generated. Finally a correlation has been developed for predicting the pressure pulse in terms of the just mentioned parameters. The individual effect of the various operating parameters and geometric parameters, namely, the diameter of the hole and the percentage free area, are discussed in the subsequent subsections.

Effect of inlet pressure

From Figure 3 it can be seen that the increase in inlet pressure increases the final collapse pressure. The collapse of the cavity depends upon the rate of pressure recovery in the expansion section. The increase in the pressure upstream of the orifice increases the downstream pressure (the pressure recovery rate as well as the final recovered pressure increases) and also the energy dissipation rate, resulting in a higher permanent pressure drop across the orifice. So the collapse of the cavity becomes more violent, which results in an increase in the pressure pulse generated at the collapse of the cavity.

It also should be noted that the increase in inlet pressure (if operated with constant flow rate) increases the cavitation number. This gives an interesting relationship between cavi-
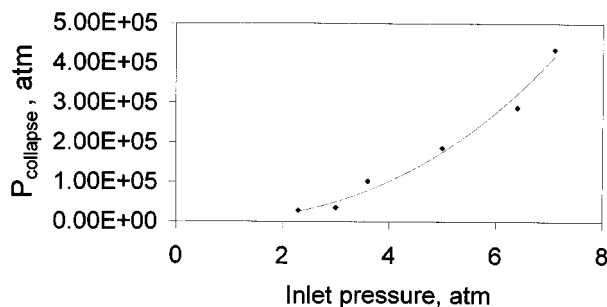

Figure 3. Variation of collapse pressure with the inlet pressure.

tation number and the generated collapse pressure. Generation of cavities generally occur near the saturation vapor pressure of the liquid at the operating temperature. An increase in the inlet pressure increases the throat pressure and decreases the cavity generation. Hence the cavitation number increases with an increase in the inlet pressure and the number of cavities generated decreases (Oba, 1986). The quantum of the total collapse pressure (collapse pressure due to a single cavity × number of cavities) can decrease beyond a certain inlet pressure, as the effect of the number of cavities will be more pronounced. Thus there is an optimum inlet pressure that should be used for getting the maximum benefits from the system (where there is a condition that the flow rate must be kept constant). Experimental studies on cell disruption using the orifice plate indicate that the percentage of cell breakage increases with the operating pressure up to a point and then decreases (Gareth and Danver, 1996). Similar results were obtained for the high-pressure homogenizer (Harrison and Pandit, 1992). An optimum pressure at which the effect due to the collapse intensity (and hence the pressure pulse generated at the cavity collapse) and number of cavities are maximum could probably exist. Experimental studies using aqueous KI decomposition as a model reaction indicated that such an optimum pressure does exist at which the iodine liberation is maximum (Shirgaonkar and Pandit, 1997; Shirgaonkar, 1997).

Vichare et al. (2000a) and Senthilkumar et al. (2000) have used a setup where the pump discharge line branches into two lines: the main line consisting of a flange that houses the orifice plate and a bypass line that controls the liquid flow through the main line. In such a case the pump discharge pressure can be adjusted by partially shutting the control valve provided in the bypass line, which will also result in an increased flow rate through the main line, though the total flow rate from the pump discharge becomes less (centrifugal pump characteristics). The extent of increase in the flow rate through the main line of the system is much larger than the increase in the pressure (Vichare et al., 2000a), and so the cavitation number of the system decreases. Thus the number of cavities that is generated also increases, thereby increasing the amount of pressure energy released due to number of pressure pulses from the system. The experimental work done on the degradation of KI in a hydrodynamic cavitation setup with orifice plates clearly confirms this fact (Vichare, 1999). Gopalkrishnan (1997) has also shown that the extent of cell disruption in a high-pressure homogenizer increases with the increase in the pressure upstream from the orifice up to a certain discharge pressure.

Effect of initial radius

Figure 4 clearly indicates that the pressure pulse generated at the time of the collapse increases with the decrease in the initial radius of the nuclei. Although it is difficult to obtain the exact size of the initial nuclei, the vapor pressure of the cavitating medium and the presence of the dissolved gases give an indication of the size of the cavity, which will be generated in the system. This effect of the initial radius on the extent of the collapse pressure generated is similar to that obtained for the case of acoustic cavitation (Gogate and Pandit, 2000). A detailed explanation of this effect and the ac-
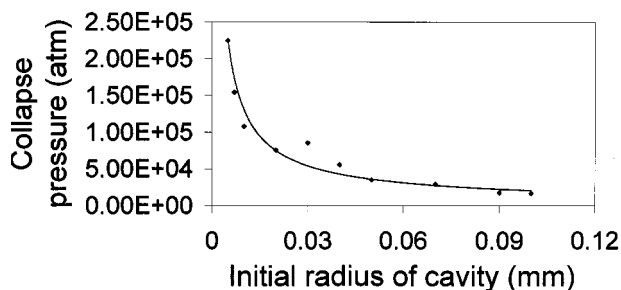

Figure 4. Variation of collapse pressure with the initial cavity radius.

count of the experimental work for supporting the observed variation is described in detail in an earlier work (Gogate and Pandit, 2000).

It also should be noted that the presence of the dissolved gases affects the final value of the collapse pressure generated. Although the initial size of the nuclei is greater (which indicates that the collapse pressure will be lower), the number of cavities generated will be higher due to the dissolved gases in the system. Thus the total amount of pressure energy released (number of cavities × pressure pulse generated by collapse of a single cavity) may be higher, thereby increasing the yield of any reaction. The present simulation work deals with a single cavity dynamic and the pressure generated due to the collapse of this single cavity. Senthilkumar et al. (2000) have clearly indicated this fact with the experiments on degradation of KI in a 50-L hydrodynamic cavitation setup with different orifice plates. The degradation rates were found to be much larger at the beginning of the experiment where the dissolved gases were present in the system. After a stabilization period of 15–20 min, complete deaeration of the system occurs, and true kinetics of the aqueous KI decomposition can be obtained showing the linear relationship between the time and the iodine yield. Thus, the true effect of the variation of the initial size of the nuclei on the generated collapse pressure is seen only after the initial stabilization of the system, and it also should be noted that the time required for the stabilization varies from system to system.

Effect of diameter of the hole

Figure 5 shows the effect of the diameter of the hole in the orifice plate on the collapse pressure pulse generated. As the diameter of the hole increases, the collapse pressure gener-
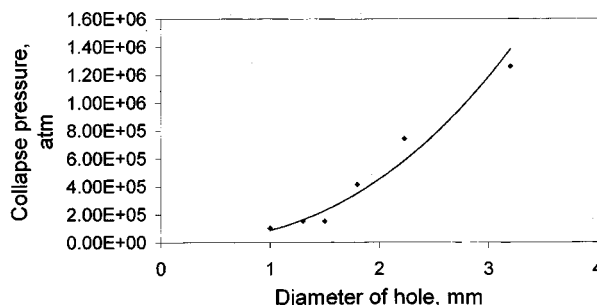

Figure 5. Variation of collapse pressure with hole diameter in the orifice plate for the same free area.
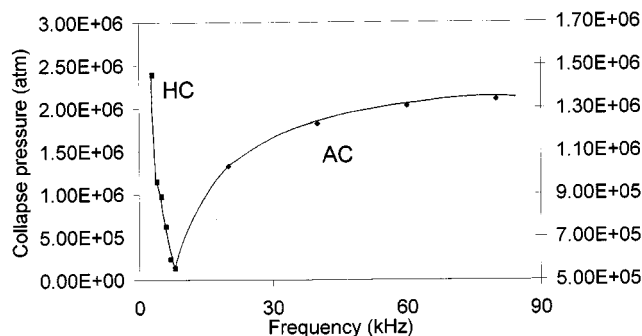
Figure 6. Variation of collapse pressure with frequency for acoustic cavitation for low frequencies.
AC-Acoustic cavitation; HC-hydrodynamic cavitation.

Figure 7. Variation of collapse pressure with the percentage free area.

ated continues to increase, which can be attributed to the way the cavitation inception number varies with the diameter of the hole. It should be noted that the effect of the hole diameter is studied for the constant percentage of free area occupied by the orifice holes and the constant inlet pressure, thereby maintaining a constant cavitation number in the system. Yan and Thorpe (1990) have shown that the cavitation inception number (defined as the cavitation number for the onset of the cavitation process) increases with the increase in the hole diameter. Thus, for a larger diameter hole, the cavitation starts at a higher cavitation number, and the extent of the cavitation also increases for the same cavitation number in the system (as long as it is below the cavitation inception number), resulting in a higher magnitude of the pressure pulse generated at the time of the collapse.

The variation in the collapse pressure with the diameter of holes obtained in the present work can also be confirmed from an illustration from the acoustic cavitation. For the same free area in the system, the frequency of the turbulence decreases with an increase in the diameter of the hole (Eq. 9 and 10). For the low frequencies of operation (<8 kHz) typically observed in the hydrodynamic cavitation, the collapse pressure generated at the time of the collapse also increases with the decrease in the frequency for the acoustic cavitation (Figure 6). It also should be noted that such low frequencies are never used in acoustic cavitation. Hence, the variation in frequency was studied only in the 20 to 200 kHz range in the earlier work of Gogate and Pandit (2000), where the collapse pressure was found to increase with an increase in the frequency. This is also a well-established fact in a number of experimental illustrations that state that the sonochemical yield increases with the increase in the frequency of operation (Petrier et al., 1992), if operating in the ultrasonic range (>20 kHz), whereas the opposite trend has been observed in the case of the hydrodynamic cavitation. The numerical scheme does indicate this variation correctly, and it is also confirmed by the experiments performed on the hydrodynamic cavitation setup using the model reaction of KI decomposition (Vichare et al., 2000a).

Effect of the free area for the flow

Figure 7 shows the variation in the collapse pressure generated with the percentage of free area available for the flow.
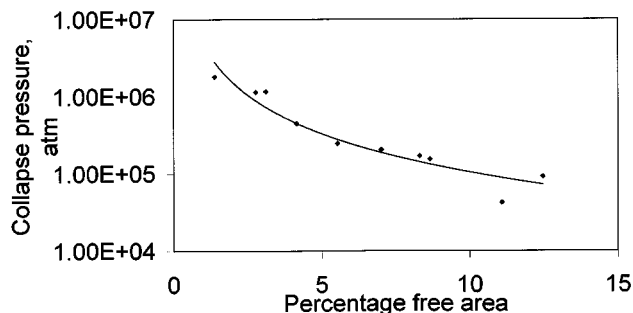
The collapse pressure is found to decrease with an increase in the percentage of free area offered by the holes in the orifice plates. The increase in the free area of the orifice results in a lower orifice velocity when the mainline flow rate is kept constant, resulting in a slower recovery of the pressure downstream from the orifice and an increase in the cavitation number. This results in a lower magnitude of the collapse pressure generated during the cavity collapse. Also the cavitation number goes on increasing with the decrease in the orifice velocity, resulting in a reduced number of cavities that will be generated in such a system. Thus the amount of pressure energy released will decrease with an increase in the free area available for the flow. Senthilkumar et al. (2000) have studied the effect of the free area by using different combinations of holes on the orifice plates. The system used was degradation of aqueous potassium iodide, resulting in the release of iodine. It was found that the amount of iodine released was greater with the plates with less available free area for flow. To give a quantitative idea, the sonochemical yield (defined as the amount of iodine liberated per unit electrical energy supplied to the system) was 4.96×10^{-9} g/J for the flow area of 25.92 mm^2 where as it was 3.79×10^{-9} g/J for the flow area of 103.67 mm^2. Vichare (1999) and Vichare et al. (2000a) have also obtained similar results for the variation of the sono chemical yield with the free area for flow on the hydrodynamic cavitation setup of 50-L capacity.

Thus, it can be said that the geometry of the vessel in terms of the percentage of free area offered for the flow and the diameter of the orifice holes affects the pressure generated at the end of the collapse of cavities. Hence care should be taken while choosing the system as per the guidelines offered in the preceding discussion so as to get maximum benefits from the hydrodynamic cavitation reactor.

Development of Correlation

The collapse pressure generated is found to be a function of the inlet pressure, initial radius of the nuclei, the diameter of the hole, which affects the frequency of turbulence for the same free area, and the percentage of free area available for the flow, which decides the liquid flow rate through the orifice. The first three parameters resemble the operating conditions in the system, and are quite similar to the intensity and frequency of ultrasound and the initial radius of the nuclei in the acoustic cavitation case. The percentage of free
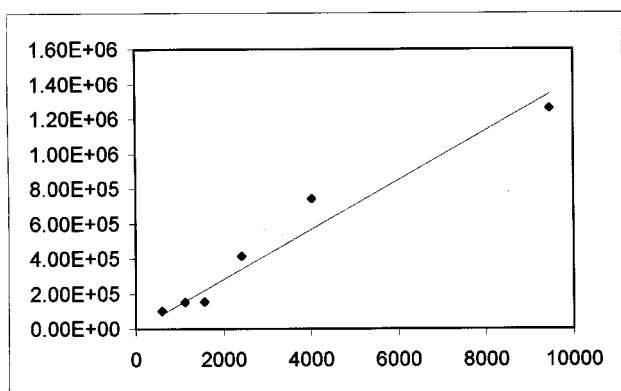
A: percentage free area = 6.93 %
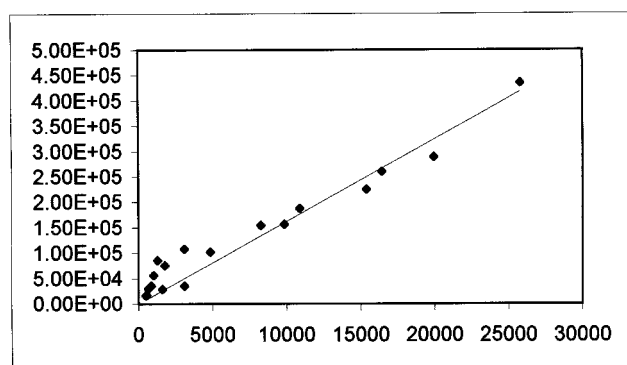
B: percentage free area = 9.12 %

Figure 8. Correlation for collapse pressure: estimation of constant C_1 for different free areas.

Figure 9. Correlation for collapse pressure: curve fitting for the constant C_1 with percentage free area.

area (resembling a system property) also affects the collapse pressure, and hence has been included in the proportionality constant, C_1. It should be noted that the diameter of the hole affects the frequency of the turbulence for the same value of the free area, and has been considered in the group of operating parameters. Thus the correlation of the following type has been developed in the present work:

$$P_{\text{collapse}} = C_1 \text{function}(P_i,\ R_o, \text{ and } d_o).$$

Figures 8 and 9 show the stepwise development of the correlation for the collapse pressure. Figure 8 gives a plot of the P_{collapse} with $(P_i)^a\, (R_o)^b\, (d_o)^c$, where the exponents a, b, and c are obtained from Figure 3, 4, and 5. The values of the exponents obtained are given as follows:

$$a = 2.46, \qquad b = -0.80, \qquad \text{and} \qquad c = 2.37.$$

It is worthwhile at this stage to compare the exponents over various parameters with those reported in our earlier work (Gogate and Pandit, 2000). If we compare the exponent over the initial pressure (2.46) with that over the acoustic intensity (-0.17), we can see the advantage of the hydrodynamic cavitation. Since the driving pressure in the case of the acoustic cavitat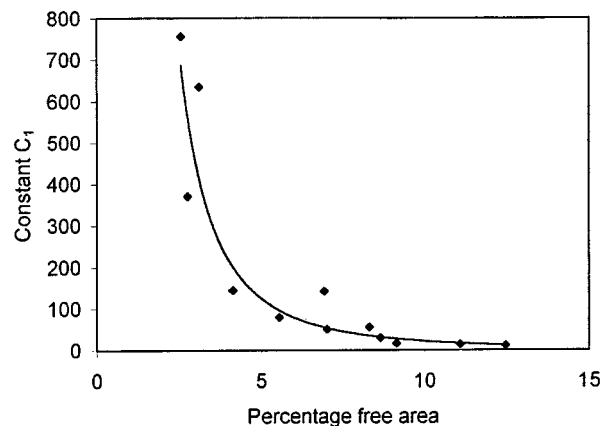ion is proportional to $I^{1/2}$, the driving pressure dependence on the collapse pressure is very small ($\cong -0.1$) compared to the exponent of 2.46 in the present case. This indicates that the hydrodynamic cavitation converts the fluid pressure energy (driving pressure field) into cavitational collapse pressures much more efficiently than does acoustic cavitation. This fact emerges very clearly from earlier experimental results as well (Save et al., 1997; Gopalkrishnan, 1997), where the cavitational yield per unit electrical energy consumed is significantly higher in the hydrodynamic cavitation case (almost 3 to 5 times; Senthilkumar et al., 2000).

The exponent for the initial cavity radius also indicates a similar behavior. The lower negative exponent (-0.8 as against -1.88) also indicates that, in the case of hydrodynamic cavitation, the collapsing cavity makes a larger contribution to the pressure pulse, indicating higher cavitational efficiency (energy released by the cavity collapse per unit work done on the cavity for its growth). Independent energy efficiency analysis of a single cavity (Vichare et al., 2000b) also supports this conclusion.

The variation in the exponents for d_o and frequency (synonymous with hydrodynamic and acoustic cavitation case) were discussed already in the previous sections.

Figure 9 is a plot of variation in the term collapse pressure/ $((P_i)^a\, (R_o)^b\, (d_o)^c)$ with the free area. Figure 9 gives the constant C_1 as a function of free area available for the flow in the system. The best-fit equation within the specified confidence limits ($R^2 > 90\%$) from Figure 9 is as follows:

$$C_1 = 7{,}527\,(A)^{-2.55}.$$

Thus the final correlation developed for the hydrodynamic cavitation is as follows:

$$P_{\text{collapse}} = 7527\,(A)^{-2.55} * \left\{ (R_o)^{2.46} (r_i)^{-0.80} (d_o)^{2.37} \right\}.$$

The preceding correlation uses the initial cavity size in mm, inlet pressure in atomspheres, and the diameter of the hole in the orifice plate in mm, while the collapse pressure is given in atmospheres and is developed for the following range of parameters:

Initial cavity size = 0.01 to 0.1 mm
Inlet pressure = 1 to 8 atm
Diameter of the orifice = 1 to 10 mm
Percentage of free area of the holes = 1–20%

The developed correlation is simple to use and valid over the range of parameters that are commonly used in the hydrodynamic cavitation applications. The development of the correlation is based on numerical results obtained from the solution of the theoretical equations, that is, the Rayleigh-Plesset equation for bubble wall velocities up to 1,500 m/s and the equation that considers the effect of the compressibility of the medium (equation of Tomita and Shima, 1986) beyond these velocities. Thus, it can be said that the correlation can be used for the design of a hydrodynamic setup for all kinds of applications using the orifice as the system for generating the hydrodynamic cavitation where rigorous numerical solutions may not be feasible.

It should be noted, however, that the preceding correlation is just an indication of the magnitude of the pressure pulse generated in the hydrodynamic cavitation reactor. In general, the cavitational yield of the process can be expressed as follows:

$$\text{Cavitational yield} = K\left(P_{\text{collapse}} \right)^{w},$$

where the constant, K, and the exponent, w, depend on the reactor geometry and operating parameters, and also on the type of reaction that is being carried out. It may happen that even if the pressure pulse generated at the collapse of the cavity is large, the effective cavitational yield could decrease due to the negative value of the exponent w, depending on the type of the reaction considered. This issue has been discussed in detail in our earlier work (Gogate and Pandit, 2000).

Conclusions

The bubble dynamics and hence the pressure generated at the collapse of the cavity is found to the dependent on the operating parameters, such as inlet pressure through the system of orifice, initial cavity size, and the diameter of the hole which affects the frequency of the turbulence existing in the reactor. The geometry of the system, that is, the percentage of free area of the holes also affects the velocity through the orifice, and thus affects the collapse pressure.

The selection of suitable operating (inlet pressure and the flow rate into the orifice setup) and geometric parameters (arrangement of holes on the orifice plates), and the vapor pressure of the cavitating media is essential for carrying out any chemical reaction using the hydrodynamic cavitation setup. Varying these conditions can significantly alter bubble behavior in hydrodynamic cavitation, thus achieving the required conditions for the specific reaction. Higher values of the inlet pressure, low initial cavity sizes, and large diameter holes, while at the same time keeping low free area for the flow, are found to result in high values for the collapse pressure.

Correlation has been developed for the prediction of the magnitude of the pressure pulse generated by the collapse of the cavity as a function of initial cavity size, diameter of holes, inlet pressure, and the percentage of free area occupied by the holes on the orifice plate. The correlation considers the effect of compressibility of the medium and is valid over the entire range of parameters, which are commonly used in the hydrodynamic cavitation applications. The developed correlation, unique in the area of cavitation reactors, can be considered a major step in the direction of the engineering design of the hydrodynamic cavitation equipment. Depending upon the collapse pressure values generated with a given set of parameters, the cavitational yield can be determined, and hence the feasibility of the existing setup for carrying out a particular application can be checked. Also the extents of cavitational yields obtained in a particular type of equipment will help in choosing the equipment for a particular application. This work is currently underway in this department.

Notation

A = percentage free area of the holes
C = velocity of sound in the liquid (m/s)
d_o = diameter of orifice (m)
$P_{collapse}$ = magnitude of pressure generated at the end of collapse of cavities (N/m²)
p_{go} = initial gas pressure (N/m²)
p_∞ = time-varying pressure field (N/m²)
$p_{(R)}$ = pressure in the liquid at the bubble wall (N/m²)
P_i = inlet pressure (N/m²)
p_i = pressure inside the bubble (N/m²)
p_o = ambient pressure (N/m²)
Δp = pressure drop across the orifice (N/m²)
r = radial distance from the bubble wall (m)
R = radius of cavity/bubble (m)
$\dot{R} = dR/dt$, bubble wall velocity (m/s)
$\ddot{R} = d^2 R/dt^2$, bubble wall acceleration (m/s²)
R_o = initial radius of the bubble (m)
R_{crit} = critical radius of the bubble/cavity (m).
t = time (s)
$\bar{v}'$ = rms velocity (m/s)
$\bar{v}_y$ = time-averaged velocity at any point in the Y-direction (m/s)
v_z = time-averaged velocity at any point in the Z-direction (m/s)
γ = specific heat ratio
σ = surface tension of liquid (N/m)
τ = time of pressure recovery (s)
μ = viscosity of liquid (Ns/m²)

Literature Cited

Chivate, M. M., and A. B. Pandit, "Effect of Hydrodynamic and Sonic Cavitation on Aqueous Polymeric Solutions," *Ind. Chem. Eng.*, **35**, 52 (1993).

Davies, J. T., *Turbulence Phenomenon*, Academic Press, New York (1972).

Flynn, H. G., *Physics of Acoustic Cavitation in Liquids in Physical Acoustics*, W. P. Mason, ed., Academic Press, New York, p. 57 (1964).

Gareth, L. C., and E. I. Danver, *The Disruption of Microbial Cells by Hydrodynamic and Ultrasonic Cavitation*, Project Rep., Univ. of Capetown (1996).

Gogate, P. R., and A. B. Pandit, "Engineering Design Methods for Cavitation Reactors: I. Sonochemical Reactors," *AIChE J.*, **46**, 372 (2000).

Gopalkrishnan, J., "Cell Disruption and Enzyme Recovery," M. Sci. Tech. Thesis, Univ. of Mumbai, Mumbai, India (1997).

Harrison, S. T. L., and A. B. Pandit, "The Disruption of Microbial Cells by Hydroydynamic Cavitation," *Int. Biotechnology Symp.*, Washington, DC (1992).

Moholkar, V. S., and A. B. Pandit, "Bubble Behaviour in Hydrodynamic Cavitation: Effect of Turbulence, *AIChE J.*, **43**(6), 1641 (1997).

Oba, R., T. Ikohagi, Y. Ito, H. Miyakura, and K. Sato, "Stochastic Behavior (Randomness) of Desinent Cavitation," *Trans. ASME, J. Fluid Eng.*, **108**, 438 (1986).

Pandit, A. B., and J. B. Joshi, "Hydrolysis of Fatty Acids: Effect of Cavitation," *Chem. Eng. Sci.*, **48**(19), 3440 (1993).

Petrier, C., A. Jeanet, J. L. Luche, and G. Reverdy, "Unexpected Frequency Effects on Rate of Oxidative Processes Induced by Ultrasound," *J. Amer. Chem. Soc.*, **114**, 3148 (1992).

Prasad Naidu, D. V., R. Rajan, K. S. Gandhi, R. Kumar, S. Chandrasekaran, and V. H. Arakeri, Modelling of Batch Sonochemical Reactor," *Chem. Eng. Sci.*, **49**, 877 (1994).

Save, S. S., A. B. Pandit, and J. B. Joshi, "Use of Hydrodynamic Cavitation for Large Scale Cell Disruption," *Chem. Eng. Res. Des.*, **75**, 41 (1997).

Senthilkumar, P., M. Sivakumar, and A. B. Pandit, "Experimental Quantification of Chemical Effects of Hydrodynamic Cavitation," *Chem. Eng. Sci.*, **55**(9), 1633 (2000).

Senthilkumar, P., and A. B. Pandit, "Modelling Hydrodynamic Cavitation," *Chem. Eng. Technol.*, **22**(12), 1017 (1999).

Shima, A., and Y. Tomita, "The Behavior of a Spherical Bubble in Mercury," Rep. 2. Rep. Inst. High Speed Mech., Tohoku Univ. Tohoku, Japan **39**, 19 (1979).

Shirgaonkar, I. Z., "Effect of Ultrasonic Irradiation on Chemical Reactions," PhD Thesis, Univ. of Mumbai, Mumbai, India (1997).

Shirgaonkar, I. Z., and A. B. Pandit, "Degradation of Aqueous Solution of Potassium Iodide and Sodium Cyanide in Presence of Carbon Tetrachloride," *Ultrasonics Sonochem.*, **4**, 245 (1997).

Sochard, S., A. M. Wilhelm, and H. Delmas, "Gas Vapour Bubble Dynamics and Homogeneous Sonochemistry," *Chem. Eng. Sci.*, **53**, 239 (1998).

Tatake, P. A., N. P. Vichare, and A. B. Pandit, "Effect of Turbulence in Hydrodynamic Cavitation," IIChE Meeting, Chandigarh, India (1999).

Tomita, Y., and A. Shima, "Mechanisms of Impulsive Pressure Generation and Damage Pit Formation by Bubble Collapse," *J. Fluid Mech.*, **169**, 535 (1986).

Vichare, N. P., "Studies in Sonochemistry and Cavitation phenomena, M. Chem. Eng. Thesis, Univ. of Mumbai, Mumbai, India (1999).

Vichare, N. P., P. R. Gogate, and A. B. Pandit, "Optimization of hydrodynamic cavitation using a model reaction," *Chem. Eng. Tech.*, (2000a).

Vichare, N. P., P. R. Gogate, P. Senthilkumar, V. S. Moholkar, and A. B. Pandit, "Energy Analysis of a Sonochemical Reactor," *Ind. Eng. Chem. Res.*, in press (2000b).

Yan, Y., and R. B. Thorpe, "Flow Regime Transitions due to Cavitation in Flow Through an Orifice," *Int. J. Multiphase Flow*, **16**, 1023 (1990).